Giant piezoresistance and its origin in Si(111) nanowires: First-principles calculations

J. X. Cao,[1,2] X. G. Gong,[3] and R. Q. Wu[1]
[1]*Department of Physics and Astronomy, University of California, Irvine, California 92697-4575, USA*
[2]*Department of Physics, Xiangtan University, 411105 Xiangtan, China*
[3]*Surface Science Laboratory (State Key) and Department of Physics, Fudan University, 200433 Shanghai, China*
(Received 10 April 2007; published 14 June 2007)

Through systematic first-principles calculations, we found extraordinarily high piezoresistance coefficients in a pristine Si(111) nanowire. This stems from interplay between the presence of two surface states with different localizations and unusual surface relaxation. Lattice compression along the axis causes switch between light and heavy surface states and, subsequently, alters the effective masses of carriers. Fascinatingly, model calculations produced main features of experimental data [R. R. He and P. D. Yang, Nat. Nanotechnol. **1**, 42 (2006)] despite much difference in wire sizes and surface conditions.

DOI: 10.1103/PhysRevB.75.233302 PACS number(s): 73.20.At, 68.65.La

One-dimensional nanowires and nanotubes exhibit extraordinary phenomena and possess an ample potential to be used in innovative nanodevices.[1–8] When wires shrink to the nanometer regime, most atoms are exposed to vacuum and the quantum confinement effect plays a major role in determining their physical properties.[9–12] Recently, it was found[13] that the piezoresistive coefficients of *p*-doped Si nanowires can be extremely high, $\pi^{\sigma}=-3550\times10^{-11}$ Pa^{-1} (more than a hundred times higher than the bulk value), a phenomenon that may find significant applications in nanomechanics and nanoelectronics. Unfortunately, it is unclear whether the enhancement of π^{σ} is intrinsic, caused by size reduction, or is simply due to oxidation. Theoretical studies using modern density-functional approaches are challenged to provide microscopic explanations and predictions for this complex phenomenon. However, to the best of our knowledge, understanding of piezoresistance effect hitherto is still at qualitative level even for bulk materials[14] and applicability of density-functional approaches toward the determination of π^{σ} has not yet been established.

In this Brief Report, we report important results of systematic density-functional studies of the piezoresistive coefficients of a Si(111) nanowire and the *p*-type bulk Si. We attained a good agreement between theory and experiment for π^{σ}_{111} of the *p*-type bulk Si, which clearly demonstrates the applicability of density-functional calculations toward the determination of piezoresistance effect. Furthermore, we predicted a giant piezoresistance effect in the pristine Si(111) nanowire and explained the results in terms of strain-induced band switch. It is fascinating that our model calculations produced all the main features of experimental data reported by He and Yang,[13] despite much difference in wire sizes and surface conditions. These insights are imperative for understanding piezoresistive properties of semiconductors and nanoentities.

We selected a pristine Si(111) nanowire as our model system to make extensive density-functional calculations feasible. As shown in Fig. 1(a), the initial geometry of the nanowire was directly taken from the bulk Si, with six equivalent (110) facets exposed to vacuum. The Vienna *ab initio* simulation package[15] (VASP) was used to solve the density-functional Kohn-Sham equation at the level of generalized gradient approximation (with the PW91 functional[16]). The ultrasoft pseudopotential for Si (Ref. 17) implemented in VASP was used for the description of electron-ion interaction. We used a three-dimensional supercell which has a period of either 1 (single cell, with 74 Si atoms) or 2 (double cell, with 148 Si atoms) *AABBCC* stacks along its axis. In the lateral plane, we tested both hexagonal and square lattices with a sufficient size of 28 Å to mimic the single wire environment. The energy cutoff for the expansion of wave function was 300 eV. Four (two for the double cell) *k* points were used to sample the essentially one-dimensional Brillouin zone. Test calculations with a larger cutoff (320 eV) and more *k* points (doubled) confirmed the convergence of results, e.g., to better than 10 meV per single cell for total energies.

To ensure the reliability of ground-state atomic structures, we optimized the length of the unit cell along its axis and positions of all atoms through the total-energy minimization procedure without any restriction in symmetry, shape, and volume. Furthermore, both initial and relaxed wires were annealed up to 875 K through *ab initio* molecular-dynamics simulations for a few thousand steps. The ground-state structure shown in Fig. 1(b) was obtained through both approaches. A snapshot of *ab initio* molecular-dynamics simulations at $T=875$ K in Fig. 1(c) is not much different from Fig. 1(b), except for the ordinary thermal expansion. Clearly, the ground-state structure displayed in Fig. 1(b) is highly stable, with which the calculated formation energy for the pristine Si(111) nanowire is as large as $E_b=E_{tot}/N-E_{atom}=-5.011$ eV/atom. Quantitatively, the length of the unit cell along the wire axis is reduced to 8.92 Å, a difference of as much as 5.77% from its bulk value, 9.466 Å. The side view

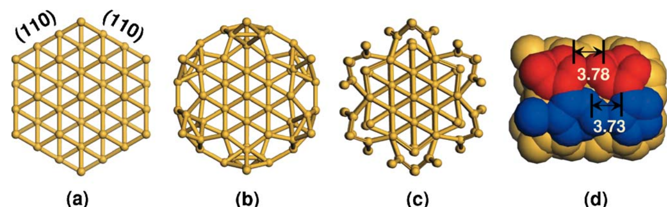

FIG. 1. (Color online) The cross sections of the Si(111) nanowire under conditions (a) initial, (b) relaxed, and (c) at $T=875$ K along with (d) the side view of the relaxed wire.

 ©2007 The American Physical Society

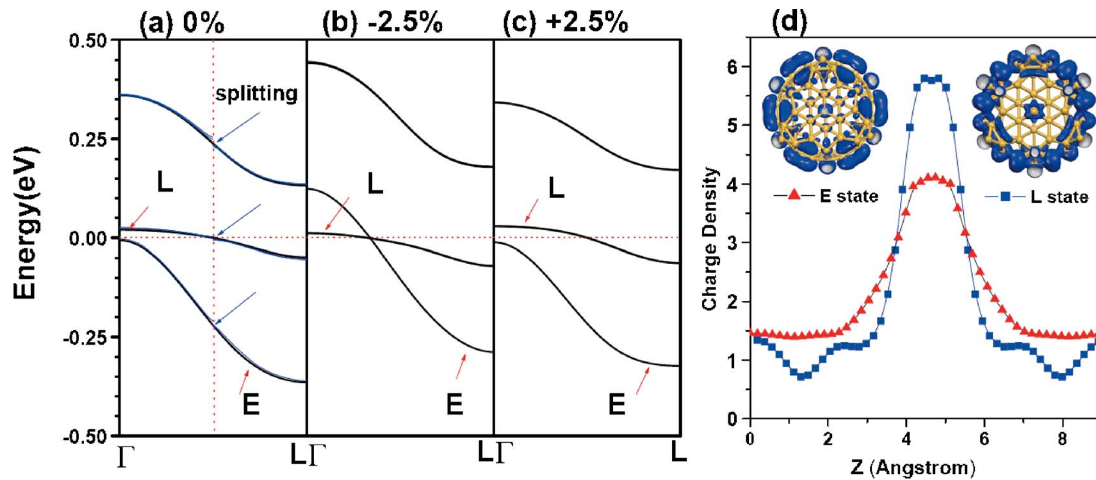

FIG. 2. (Color online) The calculated band structure of the Si(111) nanowire along the one-dimensional Brillouin zone under the (a) ambient condition, (b) 2.5% compression, and (c) 2.5% expansion. Panel (d) shows the front view and z distribution of the two surface states that are responsible for the piezoresistance effect.

in Fig. 1(d) indicates that surface Si atoms form buckled pentagons on each corner between the (110) facets and, furthermore, the pentagons dimerize along the axis.

To elucidate the transport properties, it is instructive to analyze the band structures in Figs. 2(a)–2(c). We found three surface states in the gap and two of them are near the Fermi level, i.e., the double degenerate localized L state with a very narrow dispersion ($m_L=40m_e$) and the extended E state with a wide dispersion ($m_E=0.32m_e$). Their wavefunction features are given in Fig. 2(d), where it is obvious that the E state comprises back bonds and is more uniform along the axis, whereas the L state corresponds to dangling bonds and is more localized along the axis within the region of surface pentagons. Particularly, the Fermi level intercepts with the L state right at the center of the one-dimensional Brillouin zone for the single cell. As known, this triggers the Peierls instability, and the period of nanowire should be doubled to accommodate lattice dimerization along the axis, as shown in Fig. 1(d). This additional reconstruction lowers the total energy by 21 meV per double cell and produces small gaps at the center of the Brillouin zone for the single cell. Given the characteristics of the band structure in Fig. 2(a), thin Si(111) nanowires should be poor conductors.

To explore the piezoresistance effect, we applied uniaxial strains on the nanowire in a range of ±2.5% and reoptimized the atomic structure for each strain. Strikingly, as shown in Fig. 2(b), the E state switches its position with the L state around the $\bar{\Gamma}$ point and becomes partially occupied when the negative strain is applied. This has two dramatic consequences: (1) the dimerization is removed, as manifested by results of structural relaxation for compressed wires, and (2) the E state directly contributes to transport. Moreover, the effective mass of the L state also changes due to the energy shift against the Fermi level. As a result, the inverse of the effective mass, m_0^*/m^* (with m_0^* standing for the effective mass at ambient condition), surges by a factor of 30–65 under strain >0.1%, as plotted in Fig. 3. If we assume collision time to be independent of strain, the conductance is proportional to m_0^*/m^* and hence should also increase by the same factor. Experimentally, He and Yang found that $\Delta\sigma/\sigma$ is 15 for their thin Si nanowire under a stress of 80 MPa (or roughly 0.06% of strain), in line with our theoretical results. Here, we did not consider possible incommensurate structural instability and charge-density wave in compressed Si nanowires. As was extensively discussed in the context for carbon nanotubes,[18] these effects should not affect transport properties at room temperature.

To understand why the E and L states in Si(111) nanowire switch their positions in Fig. 2(b) under compression, we separate the wire into core (from the subsurface layer) and skin (between the surface and subsurface layers) regions. It is interesting that the radius (R, defined as the average radial distance of the outmost Si atoms to the axis) and skin thickness (ΔR, defined as the difference between the radii of surface and subsurface layers) shown in Fig. 4 respond oppositely to strains. For example, while R expands under

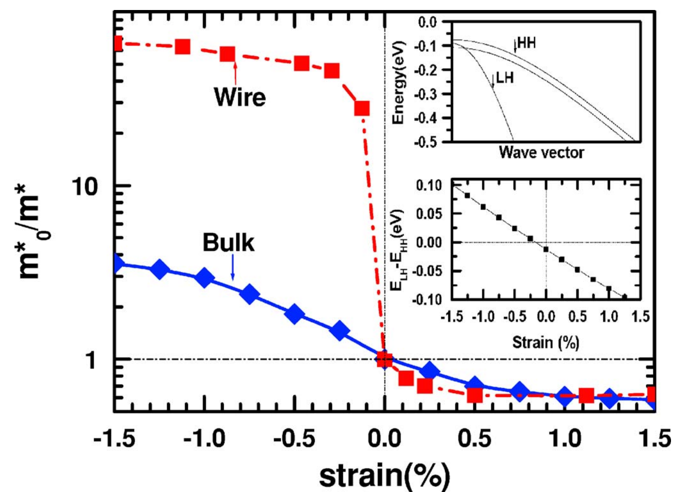

FIG. 3. (Color online) The strain-dependent effective masses of electrons (for Si nanowire) and holes (for the p-type bulk Si). The insets give the valence-band structure and energy difference between light and heavy holes at the center of the Brillouin zone of the bulk Si.

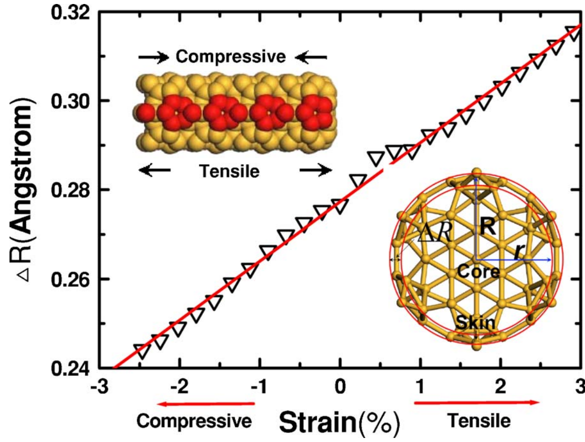

FIG. 4. (Color online) The calculated strain dependence of radius and the thickness of the skin, defined as the difference between the radii of surface and subsurface atoms. The radius for each layer is calculated as the average radial distances away from the axis.

compression as expected, ΔR shrinks due to adjustments in bond angles. Obviously, the surface layer is more rigid toward deformation. Since the E state is confined in the skin, the decrease of ΔR leads to an increase in energy of the E state and, hence, it transfers some electrons to the L state, as discussed above.

On the contrary, as shown in Fig. 2(c), positive strains barely change the electronic and atomic structures of the Si(111) nanowire, thus producing negligible alterations in its conductance. As shown in Fig. 4, tensile strains cause expansion of ΔR and should thus lower the energy of E state. However, charge transfer between E and L states is blocked since the E state is already fully occupied. The Fermi level is pinned at the L state and its occupation is also fixed for the sake of charge neutrality. As a result, the conductance of stretched Si nanowires should not be much different from that under ambient condition. The strong nonlinearity of $\Delta\sigma/\sigma$ against positive and negative strains observed from thin Si nanowires[13] is nicely reproduced in Fig. 3. Obviously, giant piezoresistance effect in Si nanowires is mainly produced by the coexistence of heavy and light surface states along with different rigidities in the skin and interior regions.

Finally, we also studied the piezoresistance effect of the p-type bulk Si for comparison to results of thick nanowires which follow bulklike behaviors. Although it was recognized that the splitting between the light hole (LH, $m_{LH}=0.138m_e$) and heavy hole (HH, $m_{HH}=0.884m_e$) at the top of valence band is the chief factor,[19–21] piezoresistance of the p-type bulk Si has never been directly calculated with modern density-functional approaches. Using a two-channel transport model, the conductivity of the p-type bulk Si can be obtained as

$$\sigma = \frac{p_{LH}e^2\tau_{LH}}{m_{LH}} + \frac{p_{HH}e^2\tau_{HH}}{m_{HH}} \approx \frac{\rho_i e^2\tau}{m^*}, \quad (1)$$

where

$$\frac{1}{m^*} = \frac{1}{p_{LH}+p_{HH}}\left(\frac{p_{LH}}{m_{LH}} + \frac{p_{HH}}{m_{HH}}\right). \quad (2)$$

At the last step in Eq. (1), we assumed that LH and HH share the same collision time τ and the sum of their densities, $p_{LH}+p_{HH}$, is equal to the concentration of dopants ρ_i. According to the definition, the piezoresistance of the p-type bulk Si along the (111) axis can be determined using

$$\pi^{\sigma}_{111} = \frac{1}{Y_{111}}\frac{d[\ln(m_0^*/m^*)]}{d\varepsilon_{111}}. \quad (3)$$

In practical calculations, we applied strains along the (111) axis (denoted as ε_{111}) with a range of ±1.5% and optimized lattice size in the perpendicular plane. The calculated Poisson's ratio ($\sigma_{111}=0.24$) and Young's modulus $[Y_{111}=(1/V)\times(d^2E_{tot}/d\varepsilon^2_{111})=177\text{ GPa}]$ agree excellently with experimental data for the bulk Si ($\sigma_{111}=-0.26$, $Y_{111}=185$ GPa).[22] Significantly, $E_{LH}-E_{HH}$ (the energy difference between the LH and HH states at the $\bar{\Gamma}$ point) decreases linearly with the strain, as shown in the insets of Fig. 3. This alters the population ratio between LH and HH according to the Boltzmann distribution, $p_{LH}/p_{HH}=A\exp[(E_{LH}-E_{HH})/k_BT]$, and subsequently leads to a change of m_0^*/m^*, as described in Eq. (2). From the strain dependence of m_0^*/m^* presented in Fig. 3 at room temperature (300 K), we have $\pi^{\sigma}_{111}=-52\times10^{-11}$ to -61×10^{-11} Pa^{-1} for $A=1/5$ and $A=1$. These results lie near the middle of experimental data for the p-type bulk Si,[23] -17 to -94×10^{-11} Pa^{-1}, and also close to results for Si nanowires with diameters larger than 300 nm.[13]

In summary, we revealed that the giant piezoresistance effect is an intrinsic feature of thin Si nanowires and explained the phenomenon through the first-principles density-functional calculations. The strain-induced band switch between two surface states, caused by unusual relaxation behavior in the surface region, is identified as the key contributor. Since the presence of surface states and quantum confinement is common in nanoentities, giant piezoresistance effect might be observed in various nanowires. This is manifested by the fact that most experimental features are reproduced in present model calculations despite differences in wire sizes and surface conditions. Extensive explorations in this direction are certainly rewarding.

This work was supported by the DOE (Grant No. DE-FG02-05ER46237). Calculations were performed on parallel computers at NERSC. J.X.C. acknowledges support from the Scientific Research Fund of Hunan Provincial Education Department (No. 05C105). X.G.G. acknowledges the support of National Science Foundation of China.

[1] N. A. Melosh, A. Boukai, F. Diana, B. Gerardot, A. Badolato, P. M. Petroff, and J. R. Heath, Science **300**, 122 (2003).
[2] A. P. Alivisatos, Science **271**, 933 (1996).
[3] L. E. Brus, P. F. Szajowski, W. L. Wilson, T. D. Harris, S. Schuppler, and P. H. Citrin, J. Am. Chem. Soc. **117**, 2915 (1995).
[4] A. J. Read, R. J. Needs, K. J. Nash, L. T. Canham, P. D. J. Calcott, and A. Qteish, Phys. Rev. Lett. **69**, 1232 (1992).
[5] D. T. Colbert, J. Zhang, S. M. McClure, P. Nikolaev, Z. Chen, J. H. Hafner, D. W. Owens, P. G. Kotula, C. B. Carter, J. H. Weaver, A. G. Rinzler, and R. E. Smalley, Science **266**, 1218 (1994).
[6] D. D. D. Ma, C. S. Lee, F. C. K. Au, S. Y. Tong, and S. T. Lee, Science **299**, 1874 (2003).
[7] X. Y. Zhao, C. M. Wei, L. Yang, and M. Y. Chou, Phys. Rev. Lett. **92**, 236805 (2003).
[8] V. Schmidt, S. Senz, and Ulrich Gosele, Nano Lett. **5**, 931 (2005).
[9] Y. Wu, Y. Cui, L. Huynh, C. J. Varrelet, D. C. Bell, and C. M. Lieber, Nano Lett. **4**, 433 (2004).
[10] J. W. Ding, X. H. Yan, and J. X. Cao, Phys. Rev. B **66**, 073401 (2002).
[11] R. Rurali and N. Lorente, Phys. Rev. Lett. **94**, 026805 (2005).
[12] R. Q. Zhang, Y. Lifshitz, D. D. D. Ma, Y. L. Zhao, Th. Frayenheim, S. T. Lee, and S. Y. Tong, J. Chem. Phys. **123**, 144703 (2005).
[13] R. R. He and P. D. Yang, Nat. Nanotechnol. **1**, 42 (2006).
[14] P. Kleimann, B. Semmache, M. Le Berre, and D. Barbier, Phys. Rev. B **57**, 8966 (1998).
[15] G. Kresse and J. Furthmuller, Comput. Mater. Sci. **6**, 15 (1996).
[16] J. P. Perdew and Y. Wang, Phys. Rev. B **45**, 13244 (1992).
[17] D. Vanderbilt, Phys. Rev. B **41**, 7892 (1990).
[18] J. W. Mintmire, B. I. Dunlap, and C. T. White, Phys. Rev. Lett. **68**, 631 (1992).
[19] T. W. Tombler, C. Zhou, L. Alexseyev, J. Kong, H. J. Dai, L. Liu, C. S. Jayanthi, M. J. Tang, and S. Y. Wu, Nature (London) **405**, 769 (2000).
[20] V. H. Crespi, M. L. Cohen, and A. Rubio, Phys. Rev. Lett. **79**, 2093 (1997).
[21] R. J. Grow, Q. Wang, J. Cao, D. W. Wang, and H. J. Dai, Appl. Phys. Lett. **86**, 093104 (2005).
[22] H. J. McSkimin, J. Appl. Phys. **24**, 988 (1953); F. J. Morin and J. P. Maita, Phys. Rev. **96**, 28 (1954).
[23] C. S. Smith, Phys. Rev. **94**, 42 (1954).